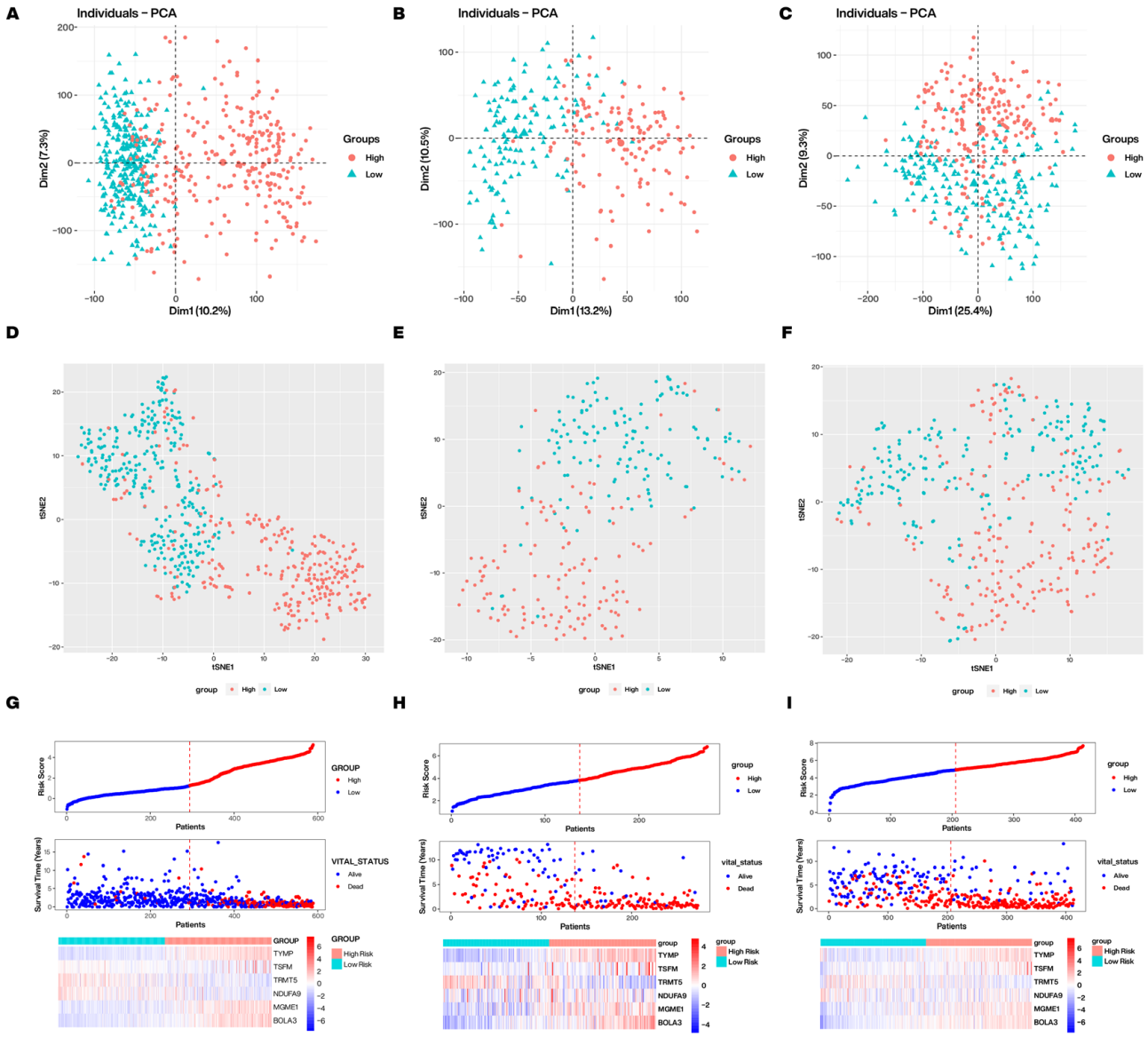

Figure S1 Statistical properties of different groups of the database. PCA, t-SNE, risk score distribution results for TCGA (A,D,G), CGGA_325 (B,E,H), and CGGA_693 (C,F,I). PCA, principal components analysis; t-SNE, t-distributed stochastic neighbor embedding; TCGA, The Cancer Genome Atlas; CGGA, Chinese Glioma Genome Atlas.

https://dx.doi.org/10.21037/tcr-23-2072

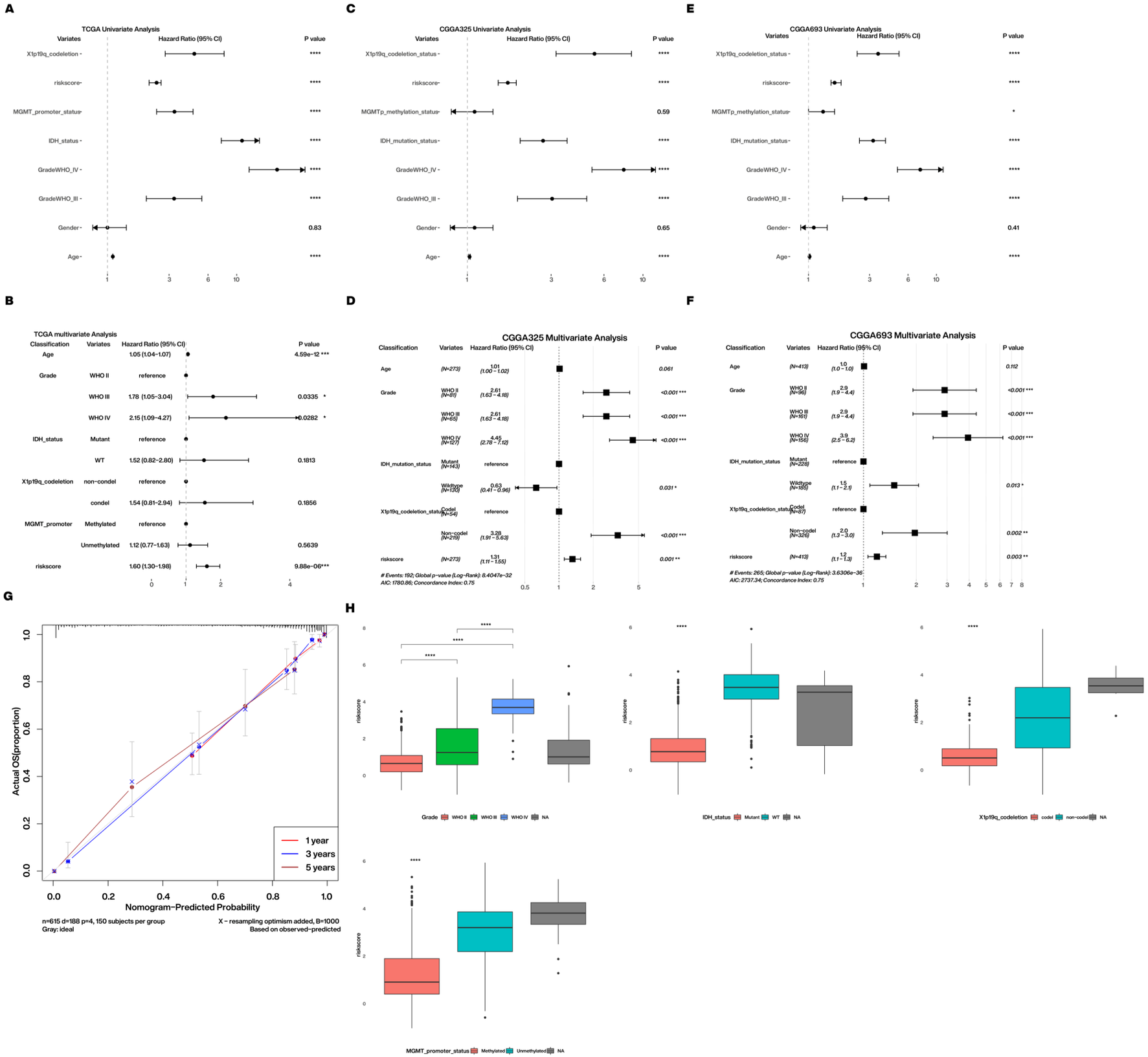

Figure S2 Results of univariate and multivariate analyses, and predictive validity of nomogram models. Univariate and multivariate Cox regression results for risk score and clinical characteristics in TCGA (A,B), CGGA_325 (C,D) and CGGA_693 (E,F). Results are expressed as a (b-c), where a is the hazard ratio (HR) and (b-c) is the 95% confidence interval. (G) The calibration plots for nomogram in TCGA. (H) The association between risk score and clinicopathological characteristics in TCGA. *, P<0.05; **, P<0.01; ***, P<0.001; ****, P<0.0001. TCGA, The Cancer Genome Atlas; CGGA, Chinese Glioma Genome Atlas.

https://dx.doi.org/10.21037/tcr-23-2072

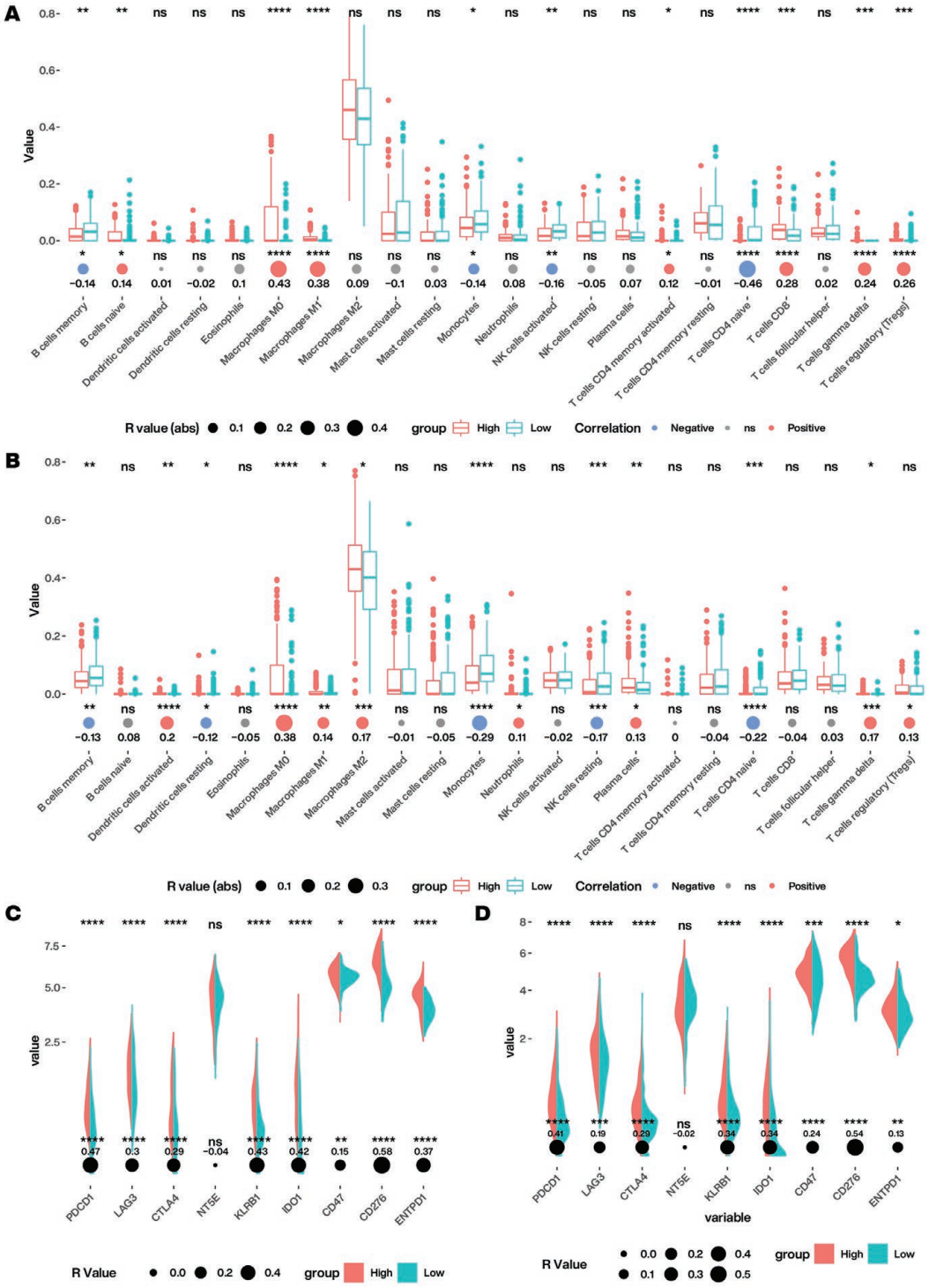

Figure S3 The landscape of immune cell infiltration status and 9 candidate immune checkpoints related gene expression between risk groups. (A,C) CGGA_325; (B,D) CGGA_693. ns, not significant; *, P<0.05; **, P<0.01; ***, P<0.001; ****, P<0.0001. CGGA, Chinese Glioma Genome Atlas.

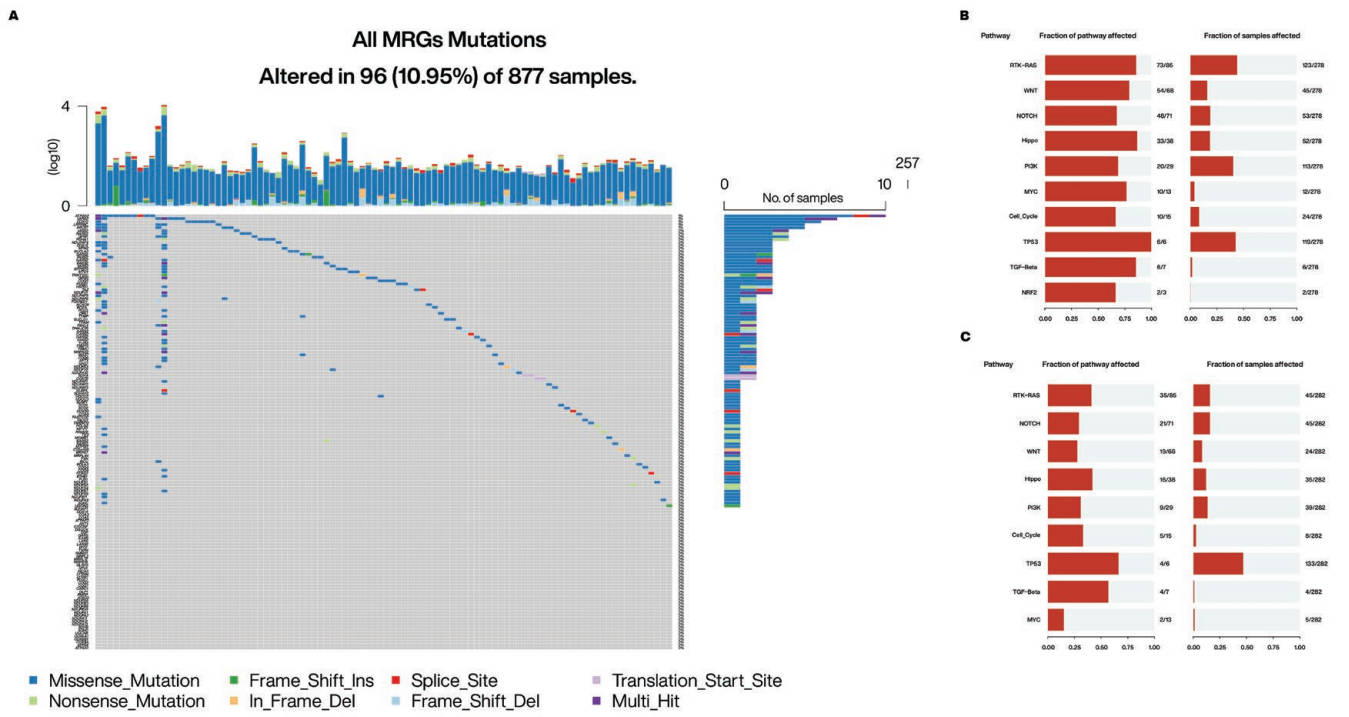

Figure S4 Supplements to the analysis results of somatic mutation. (A) The landscape of all MRGs mutations in glioma; pathways affected by mutated genes in high-risk group (B) and low-risk group (C). MRGs, mitochondrial-related genes.

https://dx.doi.org/10.21037/tcr-23-2072